applied sciences

MDPI

Article

# Catalytic Degradation of 4-Ethylpyridine in Water by Heterogeneous Photo-Fenton Process

**Nasr Bensalah [1,*], Mohammad I. Ahmad [2,*] and Ahmed Bedoui [3]**

[1] Department of Chemistry and Earth Sciences, College of Arts and Science, Qatar University, PO Box 2713, Doha, Qatar
[2] Central Laboratories Unit, Qatar University, PO Box 2713, Doha, Qatar
[3] Department of Chemistry, Faculty of Sciences of Gabes, University of Gabes, Gabes 6072, Tunisia; ahmed.bedouifsg@yahoo.fr
* Correspondence: nasr.bensalah@qu.edu.qa (N.B.); mohammad.ibrahim@qu.edu.qa (M.I.A.); Tel.: +97-444-036-540 (N.B.); +97-444-035-716 (M.I.A.)

Received: 7 November 2019; Accepted: 21 November 2019; Published: 25 November 2019


**Abstract:** In this work, the degradation of 4-ethylpyridine (4EP) in water by a heterogeneous photo-Fenton process ($H_2O_2$/$Fe_3O_4$/ultraviolet irradiation (UV)) was investigated. More rapid and effective 4EP degradation was obtained with $H_2O_2$/$Fe_3O_4$/UV than Fenton-like ($H_2O_2$/$Fe_3O_4$) and UV/$H_2O_2$, which is due to the larger production of hydroxyl radicals from the chemical and photolytic decomposition of $H_2O_2$. The operational conditions were varied during 4EP degradation experiments to evaluate the effects of pH, catalyst, concentration, and temperature on the kinetics and efficiency of $H_2O_2$/$Fe_3O_4$/UV oxidation. Under optimal conditions (100 mg/L 4EP, [$H_2O_2$] = 1000 mg/L, $Fe_3O_4$ = 40 mg/L, pH = 3 and room temperature, 300 rpm), 4EP was totally declined and more than 93% of the total organic carbon (TOC) was eliminated. Liquid chromatography analysis confirmed the formation of aromatic and aliphatic intermediates (4-hydroxypyridine, 4-pyridone, malonic, oxalic, and formic acids) that resulted in being mineralized. Ion chromatography analysis demonstrated the stoichiometric release of $NH4^+$ ions during 4EP degradation by heterogeneous photo-Fenton oxidation. The reuse of the heterogeneous catalyst was evaluated after chemical and heat treatment at different temperatures. The heat-treated catalyst at 500 °C presented similar activity than the pristine $Fe_3O_4$. Accordingly, heterogeneous photo-Fenton oxidation can be an alternative method to treat wastewaters and groundwater contaminated with pyridine derivatives and other organic micropollutants. The combination of heterogeneous photo-Fenton oxidation with classical biological methods can be proposed to reduce the overall cost of the treatment in large-scale water treatment plants.

**Keywords:** pyridine derivatives; catalyst; Fenton oxidation; UV irradiation; hydroxyl radicals; degradation

## 1. Introduction

Pyridine derivatives are synthetic compounds that are commonly used in the production of commercial products such as food aromas, paints, dyes, rubber products, waterproof fabrics, coatings, pesticides, fungicides, and antioxidants [1–3]. Pyridine derivatives include mainly alkyl pyridines, halogenated pyridines, and amino-pyridines, which have been largely used as the basic raw materials for the manufacturing of industrial solvents, agriculture herbicides, and pesticides. 4-ethylpyridine (4EP) is among the pyridine derivatives utilized in coking, chemical synthesis, pharmaceutical, and pesticide industries [4–8]. It is characterized by its high toxicity and risk of carcinogenicity, and can pose human health and environment concerns [5–9]. In addition, 4EP is soluble in water, very stable

and difficult to biodegrade [10–14]. It is largely spread across the environment due to its extensive use and can contaminate groundwater and surface waters [8–14]. The conventional biological remediation process treatment methods are not able to completely remove 4EP from contaminated water [15–17]. The search for a treatment method to eliminate it from water, transform it to a biocompatible form, or lessen its toxicity is urgently desired.

Particularly, advanced oxidation processes (AOPs) showed high potential to degrade various bioresistant and hazardous organic pollutants in water [18–20]. These processes are capable of mineralizing several types of organic pollutants, including phenols, polyphenols, pesticides, pharmaceuticals, etc. [19,21]. The great efficacy of AOPs is mainly due to the generation of powerful oxidizing radicals, mainly hydroxyl radicals ($HO^{\bullet}$) [22,23].

These unstable radical species with a very short lifetime and a high standard potential ($E^{\circ}$ = 2.80 V/SHE) react immediately and non-selectively with organic pollutant molecules leading to total mineralization into $CO_2$, $H_2O$, and other inorganic ions, or partial transformation to substances easy to biodegrade [22–24]. In particular, photo-Fenton oxidation ($UV/H_2O_2/Fe^{2+}$) is a good option to reduce and eliminate many pollutants during wastewater treatment. It is considered as the most effective $H_2O_2$-based process in the treatment of various effluents containing highly toxic and bio-resistant organic compounds [20,25,26].

In this process, $HO^{\bullet}$ radicals generated from $H_2O_2$ decomposition by UV photolysis and by ferrous iron catalyst (Equations (1) and (2)):

$$Fe^{2+}_{aq} + H_2O_{2aq} \rightarrow Fe^{3+}_{aq} + HO^{\bullet} + H^{+}{}_{aq} \quad (1)$$

$$H_2O_{2aq} + h\nu \rightarrow HO^{\bullet} + HO^{\bullet} \quad (2)$$

However, high amounts of $Fe^{2+}$ are needed to attain complete removal of organic pollutants, which results in another environmental problem related to the discharge of treated water or sludge contaminated with iron, and it also increases the operational costs of the treatment process. Using heterogeneous iron catalysts can solve these economic and environmental problems since the catalyst can be assembled at the end the treatment and recycled many times [27–34]. Natural and synthetic magnetite, $Fe_3O_4$, containing both $Fe^{2+}$ and $Fe^{3+}$ catalytic sites, was successfully used to degrade organic pollutants [34–39]. The decomposition of $H_2O_2$ on the surface $Fe_3O_4$ produces radicals species ($HO_2^{\bullet}$ and $HO^{\bullet}$) that are capable of degrading any type of organic pollutant according to the following equations (Equations (3) and (4)):

$$\| Fe^{3+}_{Surface} + H_2O_2 \rightarrow \| Fe^{2+}_{Surface} + HOO^{\bullet} + H^{+} \quad (3)$$

$$\| Fe^{2+}_{Surface} + H_2O_2 \rightarrow \| Fe^{3+}_{Surface} + HO^{\bullet} + H^{+} \quad (4)$$

The catalyst can be easily collected by magnet or by filtration and be regenerated and recycled for additional experiments. The efficiency of natural and synthetic $Fe_3O_4$ heterogeneous catalysts in the production of $HO^{\bullet}$ radicals by decomposition of $H_2O_2$ was demonstrated by several authors [34–39]. Furthermore, it was also reported that the combination of Fenton-like oxidation using $Fe_3O_4$ as a catalyst with UV irradiation enhanced the efficiency of the whole process [34–36]. The hydroxyl radicals produced by photo-decomposition of $H_2O_2$ (Equation (2)) attack the molecules adsorbed on the surface of the catalyst degrading them and make more catalytic sites available. The formation of stable iron (III)-carboxylate complexes would be minimized and higher mineralization yield would be obtained.

The aim of this present work was to investigate the degradation of 4EP in water by heterogeneous photo-Fenton oxidation using $Fe_3O_4$ as a catalyst and to demonstrate the reuse of the heterogeneous catalyst several times in photo-Fenton oxidation. Different methods of activation of the catalyst were used, including acid treatment, drying at room temperature, and heat treatment at 100 °C, 250 °C, and 500 °C. The effects of principal experimental parameters, such as initial pH, $Fe_3O_4$

dose, $H_2O_2$, and 4EP concentrations on the performance of 4EP degradation and mineralization by heterogeneous photo-Fenton process were evaluated. 4EP and the formation of organic intermediates during degradation experiments were monitored by high-performance liquid chromatography (HPLC). The formation of inorganic nitrogen species ($NO_3^-$, $NO_2^-$, $NH_4^+$) as mineralization end-products were monitored by ion chromatography. Accordingly, a simple 4EP degradation mechanism by the heterogeneous photo-Fenton process was proposed.

## 2. Materials and Methods

### 2.1. Chemicals

4EP ($C_6H_5NO_2$) and $H_2O_2$, 30% (*w*/*w*) solution were purchased from Fluka. Other chemicals such as $Fe_3O_4$ (powder, particles size < 5 μm, 95%), $H_2SO_4$, NaOH and $Na_2SO_3$ were of analytical grade Sigma-Aldrich chemicals. The preparation of synthetic solutions was performed using deionized water with resistivity > 18 MΩ $cm^{-1}$ at 25 °C from a Millipore Milli-Q system. The eluents ($CH_3CN$ and $CH_2O$) used in HPLC analysis were of HPLC grade and received from Merck.

### 2.2. Analytical Methods

Total organic carbon (TOC) was measured by an Analytik Jena TOC analyzer to follow up the mineralization of 4EP in aqueous solutions. An ion chromatograph (Shimadzu LC-20A) equipped with a Shodex IC YK-421 column was used to analyze the inorganic ions (nitrate, nitrite, and ammonium) formed during the mineralization. A mixture of 5.0 mM tartaric acid, 1.0 mM dipicolinic acid, and 24.3 mM boric acid was used as the eluent in isocratic mode (1.0 mL $min^{-1}$). The analysis of 4EP and its degradation intermediates was carried out using liquid chromatography (HPLC–UV), with an Agilent 1100 unit at constant temperature (25 °C) equipped with a Phenomenex Gemini 5 μm C18 column. The wavelength of the UV detector was performed at 260 nm. A lineal gradient chromatographic elution was used by initially running 10% of Solvent B ascending to 100% in 40 min. Solvent A was composed of 25 mM of formic acid water solution, and Solvent B was acetonitrile. All the samples withdrawn from the treated solutions underwent a filtration aver 0.20 μm membranes before analysis. Absorbance measurements and absorption spectra of 4EP aqueous solutions were recorded using a Shimadzu UV-1603 spectrophotometer in quartz cells (1 cm). The pH was determined using an InoLab WTW pH-meter.

### 2.3. Photo-Fenton Experiments

The photochemical experiments were carried out in the reactor equipped with a mercury vapor UV lamp (Heraeus Noblelight) (YNN 15/32) with a power input of 125 W, a magnetic stirrer, and a thermometer. The photo-reactor (Pyrex) of 2 L capacity was placed in the first part. The lamp was located in an axial position submerged in a vertical immersion tube contained in a vertical cooling tube and immersed in the solution. Water was circulated between the lamp and glass vessel. The experiment was mounted on a magnetic stirrer. In this work, mercury vapor lamps emit UV irradiation at 254 nm, which is mainly absorbed by $H_2O_2$. The volume of 4EP wastewater was 1 L. The pH of the solution was adjusted to the desired values by addition of sodium hydroxide or sulfuric acid. After pH adjustment, a given weight of $Fe_3O_4$ was added. The magnetite was mixed very well with the solution of 4EP wastewater to form a homogeneous suspension. After the light of the lamp, a precise amount of 30% hydrogen peroxide was mixed with the suspension formed. At certain time intervals, samples of 10 mL volume were taken from the solution. The reaction was quenched with $Na_2SO_3$ and then analyzed immediately to determined pH. The samples were filtered through 0.20 μm nylon filters and analyzed for inorganic ions, TOC, target compounds and intermediates, and UV–VIS absorbance at a wavelength of λ = 260 nm.

## 3. Results and Discussions

### *3.1. Comparative Performance of $H_2O_2/Fe_3O_4$, UV/$H_2O_2$, and UV/$H_2O_2/Fe_3O_4$ Processes*

In order to highlight the importance of combining the Fenton-like process and UV irradiation, the performance of single and combined processes, including UV irradiation, $H_2O_2$ oxidation ($H_2O_2$ = 1000 mg/L), $Fe_3O_4$ adsorption ($Fe_3O_4$ = 40 mg/L), $H_2O_2/Fe_3O_4$ ($Fe_3O_4$ = 40 mg/L and $H_2O_2$ = 1000 mg/L), UV/$H_2O_2$, and UV/$H_2O_2/Fe_3O_4$ ($Fe_3O_4$ = 40 mg/L and $H_2O_2$ = 1000 mg/L) in treating 4EP aqueous solutions were compared. Figure 1 presents 4EP removals from 100 mg/L 4EP aqueous solutions at pH 3 using the single and combined processes over 60 min. For the single processes (UV irradiation, $H_2O_2$ oxidation, $Fe_3O_4$ adsorption), 4EP removals did not exceed more than 6% indicating the slowness of the reactions involved in the elimination of 4EP from water. UV irradiation alone does not have enough energy to rupture all the chemical bonds in 4EP molecules. $Fe_3O_4$ active adsorption surface sites adsorb only a few 4EP molecules because of its low specific area. Even $H_2O_2$ oxidation showed a higher 4EP removal compared to the two other single processes (UV irradiation and $Fe_3O_4$ adsorption), its power is not sufficient to oxidize large 4EP molecules in water.

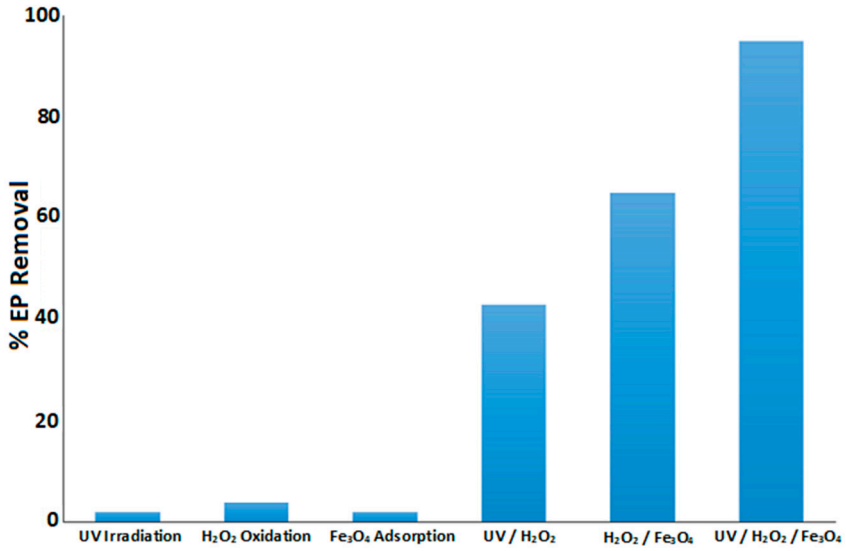


**Figure 1.** The percent of EP removal at the end of the treatment of 100 mg/L EP aqueous solutions at pH = 3, and 25 °C, under 300 rpm stirring by UV irradiation, $Fe_3O_4$ (40 mg/L) adsorption, $H_2O_2$ (1000 mg/L) oxidation, UV/$H_2O_2$ process ($H_2O_2$ = 1000 mg/L), Fenton-like process ($Fe_3O_4$ = 40 mg/L and $H_2O_2$ = 1000 mg/L), and the heterogeneous photo-Fenton process ($Fe_3O_4$ = 40 mg/L and $H_2O_2$ = 1000 mg/L).

However, combined processes showed higher 4EP removals than single processes. The heterogeneous photo-Fenton (UV/$H_2O_2/Fe_3O_4$) process achieved the highest 4EP removal of 95%, however, the Fenton-like ($H_2O_2/Fe_3O_4$) and UV/$H_2O_2$ processes removed 65% and 43% 4EP from water within 60 min. For further investigations of 4EP degradation kinetics using the combined processes, the changes of 4EP concentration with time are plotted and presented in Figure 2 for each of the combined processes. This figure shows that the 4EP concentration declined with time for all combined processes indicating the degradation of 4EP molecules. The highest 4EP removals were measured after 120 min, 180 min, and 360 min for the heterogeneous photo-Fenton (99%), Fenton-like (95%), and UV/$H_2O_2$ (94%) processes, respectively. The degradation of 4EP in water by each of the combined processes follows pseudo-first-order kinetics as confirmed by the linear plots of $Ln[4EP]_0/[4EP]_t$ vs. time (inset of Figure 2). Pseudo-first-order rate constants of 0.007 $min^{-1}$, 0.02 $min^{-1}$, 0.05 $min^{-1}$ are calculated for UV/$H_2O_2$, Fenton-like, and heterogeneous photo-Fenton

processes, respectively. These results demonstrate that heterogeneous photo-Fenton process is more rapid and more efficient than UV/$H_2O_2$ and Fenton-like processes in degrading 4EP in water. The higher effectiveness of the heterogeneous photo-Fenton (UV/$H_2O_2$/$Fe_3O_4$) oxidation can be due to the larger production of hydroxyl radicals from both the catalytic decomposition of $H_2O_2$ by $Fe_3O_4$ catalyst, and the photo-decomposition of hydrogen peroxide by irradiation UV.

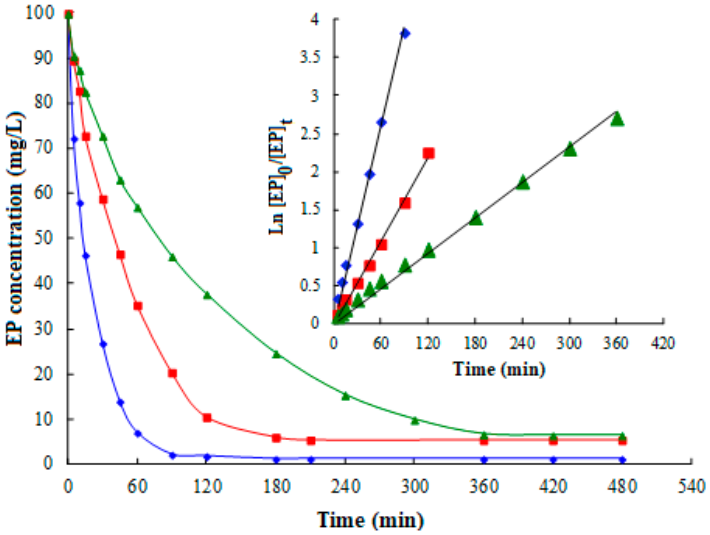


**Figure 2.** Kinetics of EP degradation (100 mg/L EP, at pH = 3, 25 °C, 300 rpm stirring) via: (-▲-) the UV/$H_2O_2$ process ($H_2O_2$ = 1000 mg/L); (-■-) the Fenton-like process (($Fe_3O_4$= 40 mg/L and $H_2O_2$ = 1000 mg/L)) and (-♦-) the heterogeneous photo-Fenton process ($Fe_3O_4$= 40 mg/L and $H_2O_2$ = 1000 mg/L). Inset: Pseudo-first-order kinetics plots.

### *3.2. Detailed Onvestigations of the Degradation of 4EP by the Heterogeneous Ohoto-Fenton Process*

The comparative experiments demonstrated the effectiveness of the heterogeneous photo-Fenton process in degrading 4EP in water. However, taking into account the fact that the treatment of 4EP by the heterogeneous photo-Fenton process aims to mineralize it into $CO_2$, $H_2O$, and $NO_3^-$ (or $NH_4^+$) or to transform it into easily biodegradable compounds, further experiments are needed to optimize the operating conditions targeting the integration of this method in larger applications than the lab scale. For that purpose, a series of experiments were conducted to examine the effects of some experimental parameters on the kinetic and the efficiency of the treatment of 4EP synthetic wastewaters by UV/$H_2O_2$/ $Fe_3O_4$ process. Initial pH, $Fe_3O_4$ dose, and $H_2O_2$ and 4EP concentrations are the experimental parameters selected to be optimized to reach the highest yields of 4EP degradation and mineralization.

Fenton and photo-Fenton reactions are strongly pH-dependent as reported in the literature [40–43]. Especially, it is well reported that the initial pH conditions significantly influence the production of hydroxyl radicals [20,43–46]. To examine the effect of initial pH on the treatment of aqueous solutions containing 100 mg/L of 4EP by the heterogeneous photo-Fenton process, the initial pH values was varied in the range between 3 and 9 using 1000 mg/L $H_2O_2$ and 40 mg/L $Fe_3O_4$ at room temperature and a stirring rate under 300 rpm. The effect of the initial pH on TOC removal is given in Figure 3. This figure shows that TOC decreased from the beginning of the treatment for all initial pH values. The highest TOC removal was obtained at pH 3. Increasing pH from 3 to 5, to 7, and then to 9 decreased TOC removal. During the treatment of 4EP aqueous solutions by the heterogeneous photo-Fenton process, TOC declined from 56 mg C/L to 2.1 mg C/L at pH 3.0, to 12.3 mg C/L at pH 5.0 and 17.5 mg C/L at pH 7.0 and 9.0 after 360 min. This indicates that more than 96% of TOC removal was achieved at pH 3.0, while TOC removals between 68% and 78% were calculated for the other initial pH values. The TOC removal during the treatment of 100 mg/L 4EP aqueous solution using the homogeneous

photo-Fenton process (UV/$H_2O_2$/$Fe^{2+}$: 1000 mg/L $H_2O_2$, 10 mg/L $Fe^{2+}$ (similar amount of iron used with $Fe_3O_4$)) achieved 98% at pH 3.0, 72% at pH 5.0, 56% at pH 7.0, and 37% at pH 9.0 after 360 min (data not shown here). These results demonstrated that the initial pH affects the efficiency of the treatment for both heterogeneous and homogeneous photo-Fenton processes; however, the lower effect on TOC removal was observed with the heterogeneous photo-Fenton. The difference between the heterogeneous and homogeneous photo-Fenton processes can be related to the slower regeneration of the homogeneous catalyst ($Fe^{2+}$) at pH > 5 because of the precipitation of $Fe(OH)_3$. In addition, the decrease in the TOC removal in both the homogeneous and heterogeneous photo-Fenton processes could be due to the acceleration of auto-decomposition of $H_2O_2$ leading to the lower production of hydroxyl radicals [20,42–45]. The analysis of iron leached from the $Fe_3O_4$ solid catalyst is needed in this case to have an idea about the effect of the pH on the dissolution of iron during the treatment at different initial pH values.

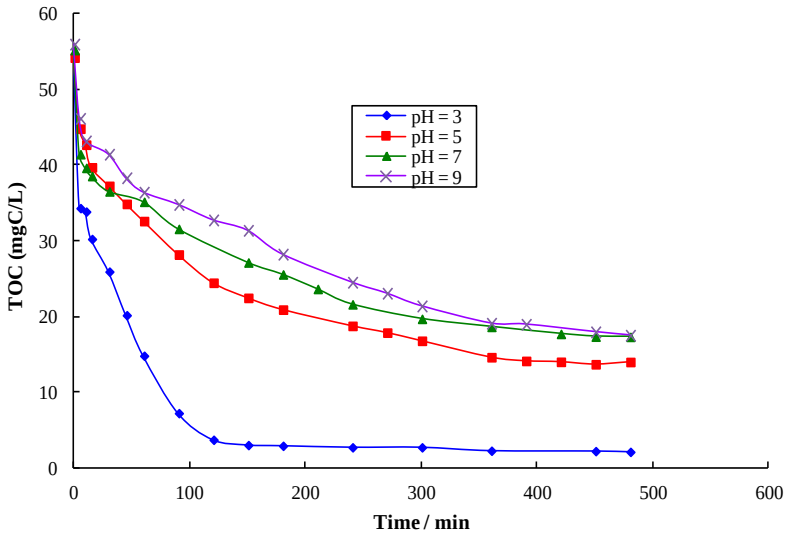


**Figure 3.** Influence of initial pH on TOC changes with time during heterogeneous photo-Fenton treatment of 100 mg/L EP aqueous solutions. Experimental conditions: 1000 mg/L $H_2O_2$, 40 mg /L $Fe_3O_4$, pH 3–9, T = 25 °C, 300 rpm.

Table 1 illustrates the results of the analysis of iron by ICP–OES during the heterogeneous photo-Fenton treatment in the same conditions as Figure 3. The results show that small amounts of iron were measured in solution at neutral and alkaline media (0.63 and 0.14 mg/L at pH 7 and pH 9); however, 25% and 17% iron was dissolved at pH 3 and pH 5 (9.65 mg/L iron are contained in 40 mg/L $Fe_3O_4$) at the end of the treatment. Based on the data obtained in the present study, an initial pH between 3.0 and 5.0 can achieve higher TOC removal than 75% using the heterogeneous photo-Fenton process with less than 20% of the iron being leached from the $Fe_3O_4$ solid catalyst.

**Table 1.** Analysis of dissolved iron during the treatment of 100 mg/L EP aqueous solutions by the heterogeneous photo-Fenton using 40 mg/L $Fe_3O_4$ and 1000 mg/L $H_2O_2$ at pH 3 under 300 rpm stirring and 25 °C.

| Time | pH = 3.0 | pH = 5.0 | pH = 7.0 | pH = 9.0 |
|---|---|---|---|---|
| 0 min | 0.08 mg/L Fe | 0.05 mg/L Fe | ND | ND |
| 60 min | 0.58 mg/L Fe | 0.19 mg/L Fe | 0.05 mg/L Fe | 0.01 mg/L Fe |
| 120 min | 1.96 mg/L Fe | 1.43 mg/L Fe | 0.11 mg/L Fe | 0.02 mg/L Fe |
| 180 min | 2.13 mg/L Fe | 1.51 mg/L Fe | 0.45 mg/L Fe | 0.05 mg/L Fe |
| 360 min | 2.37 mg/L Fe | 1.62 mg/L Fe | 0.63 mg/L Fe | 0.14 mg/L Fe |

The catalyst dose is considered as a determining parameter for the production of radical oxidant species from the $H_2O_2$ decomposition (Equations (1) and (3)) [44–46]. Iron(II)/Iron(III) in solid form or in solution are excellent catalysts to decompose $H_2O_2$ efficiently into hydroxyl radicals $HO^{\bullet}$. The dose of the catalyst should be carefully adjusted to achieve high degradation yields and avoid the formation of stable iron(II)/(III) organic complexes. To evaluate the effect of the $Fe_3O_4$ catalyst, some experiments of heterogeneous photo-Fenton treatment of 100 mg/L 4EP synthetic wastewater were carried using a fixed $H_2O_2$ concentration of 1000 mg/L at pH 3, and varying the dose of $Fe_3O_4$ in the range from 0 to 100 mg/L at room temperature. The changes of TOC with time at different doses of $Fe_3O_4$ are presented in Figure 4. These results display that the TOC decreased with time for all $Fe_3O_4$ doses from the beginning of the treatment. The addition of $Fe_3O_4$ catalyst accelerated the TOC decay compared to the experiment in its absence. The increase of $Fe_3O_4$ concentration up to 40 mg/L improved the kinetics and the efficiency of the heterogeneous photo-Fenton process (87% and 96% TOC removals were calculated for 20 and 40 mg/L $Fe_3O_4$, respectively). However, higher doses of $Fe_3O_4$ than 40 mg/L decreased the efficiency of the degradation of 4EP by heterogeneous photo-Fenton process in terms of TOC removal. Using 80 and 100 mg/L $Fe_3O_4$ resulted in 85% and 74% TOC removals, respectively. It can be concluded that the most rapid TOC decay and the highest TOC removal were obtained with 40 mg/L $Fe_3O_4$.

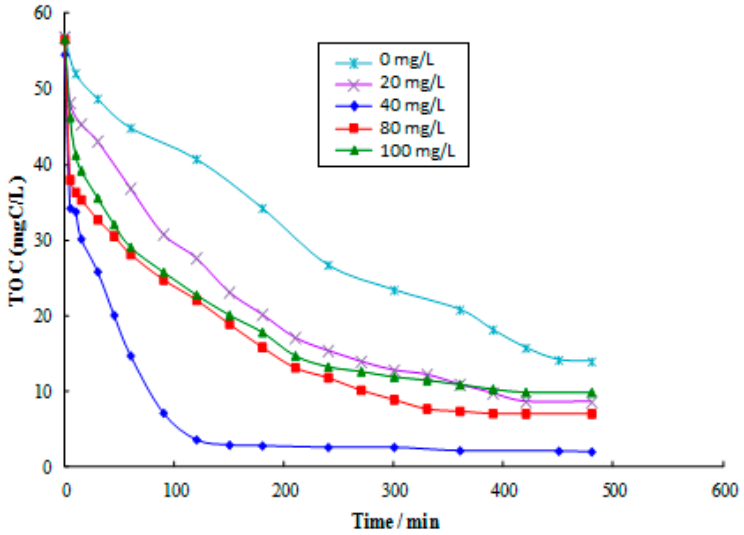


**Figure 4.** Influence of $Fe_3O_4$ dose on TOC changes with time during the heterogeneous photo-Fenton treatment of 100 mg/L EP aqueous solutions. Experimental conditions: 1000 mg/L $H_2O_2$, 0–100 mg /L $Fe_3O_4$, pH 3, T = 25 °C, 300 rpm.

These results can be explained by the acceleration of the production of radical species (mainly hydroxyl radicals), the latter can reduce preferably Fe(III) sites on the catalyst surface when higher $Fe_3O_4$ doses than 40 mg/L are added instead of degrading 4EP and its intermediates. The reuse of the catalyst was tested by the collection of the solids by magnet and washing them several times with deionized water. The collected solids were heat treated at temperatures of 105, 180, 250, and 500 °C. Table 2 presents the results of heat treatment and the reuse of the catalyst in treating 100 mg/L 4EP aqueous solutions using 1000 mg/L $H_2O_2$, 40 mg/L reused catalyst at pH 3 and under 300 rpm stirring and room temperature. The increase of the temperature of the heat treatment decreased the mass of the catalyst, which can be explained by the dehydration and the release of volatile organics adsorbed on the surface of the catalyst with possible transformation of the catalyst by oxidation/reduction reactions in presence of air. In contrast, the increase of the heat treatment temperature enhanced TOC removal, which keep values higher than 64% for the treated catalyst. The same catalyst was collected, then treated at 500 °C, and reused in treating 4EP aqueous solutions in the same conditions. TOC removals in the range of 83%–89% were measured indicating the good efficacy of the reused

catalyst. These results confirm the possible reuse of the solid catalyst for several times in heterogeneous photo-Fenton treatment of 4EP in water.

**Table 2.** Results of the reuse of the catalyst during the treatment of 100 mg/L EP aqueous solutions by the heterogeneous photo-Fenton using 40 mg/L treated catalyst and 1000 mg/L $H_2O_2$ at pH 3 under 300 rpm stirring and 25 °C.

| Heat Treatment (240 min) | Mass Collected (mg/L) | % TOC Removal (360 min) |
|---|---|---|
| T = 105 °C | 36.2 | 64 |
| T = 180 °C | 33.6 | 70 |
| T = 250 °C | 32.4 | 76 |
| T = 500 °C | 30.3 | 89 (85/87/84/86) |

The efficacy of the Fenton and photo-Fenton processes in treating wastewaters containing organic pollutants depends largely on the production of hydroxyl radicals by chemical and photochemical decomposition of hydrogen peroxide [40–42]. $H_2O_2$ is the main source of hydroxyl radicals even if little amount of $OH^\bullet$ can be formed by water photolysis. Consequently, the optimization of $H_2O_2$ initial concentration ($[H_2O_2]_0$) is fundamental to achieve a high production of hydroxyl radicals [18–20]. To examine the effect of $H_2O_2$ initial concentration on the performance of the heterogeneous photo-Fenton process, aqueous solutions containing 100 mg/L 4EP at pH 3.0 and 25 °C were treated by $H_2O_2$ initial concentration in the range of 500–2000 mg/L. The dose of $Fe_3O_4$ was calculated for each $H_2O_2$ initial concentration from the mass ratio $H_2O_2/Fe_3O_4$ fixed to 25. The results illustrated in Table 3 confirm that the efficiency of the heterogeneous photo-Fenton process depends on the $H_2O_2$ initial concentration. The results of Table 1 showed that the TOC removal increased from 86% to 93%, then it decreased to 81% after 120 min of adding 500, 1000, and 2000 mg/L of $H_2O_2$, respectively.

**Table 3.** Influence of $H_2O_2$ and EP concentrations on TOC removal during the treatment by the heterogeneous photo-Fenton process ($UV/H_2O_2/Fe_3O_4$) during 120 UV irradiation at pH 3 and under 300 rpm stirring and 25 °C.

| $[H_2O_2]_0$ (mg/L) | $[EP]_0$ (mg/L) | % TOC Removal |
|---|---|---|
| 500 | 100 | 86 |
| 1000 | 100 | 93 |
| 2000 | 100 | 81 |
| 1000 | 50 | 92 |
| 1000 | 100 | 93 |
| 1000 | 200 | 84 |

The fact that the highest TOC removal was achieved with 1000 mg/L $H_2O_2$ initial concentration is essentially due to the production of satisfactory amounts of $HO^\bullet$ radicals capable to mineralize most of the organic matter. Although, the increase of $H_2O_2$ dose to higher than 1000 mg/L would theoretically result in a larger production of $HO^\bullet$ radicals, it did not result in an enhancement of the TOC removal. This may be due to the consumption of $HO^\bullet$ radicals by excessive amounts of $H_2O_2$ (Equation 5 and 6) and the acceleration of $H_2O_2$ disproportionation into $O_2$ and $H_2O$ (Equation (7)) [42–48]:

$$HO^\bullet + H_2O_2 \rightarrow H_2O + HO_2^\bullet \quad (5)$$

$$HO^\bullet + HO_2^\bullet \rightarrow H_2O + O_2 \quad (6)$$

$$2H_2O_2 \rightarrow 2H_2O + O_2 \quad (7)$$

To evaluate the effect of 4EP initial concentration on the efficiency of the heterogeneous photo-Fenton process, pH and temperature were fixed at 3 and 25 °C, and the mass ratio $H_2O_2/Fe_3O_4$ and $H_2O_2$]/4EP were maintained constant and equal to 25 and 10, respectively. The 4EP initial concentration was varied in the range of 50–200 mg/L (see Table 3). Increasing 4EP initial concentration from 50 to 100 mg/L increased TOC removal from 87% to 93% after 120 min; while increasing the 4EP initial concentration from 100 to 200 mg/L decreased TOC removal to 84%. This is mainly due to the smaller production of radical species limited by $H_2O_2$ concentration and $Fe_3O_4$ dose for low 4EP initial concentrations and to the absorption of UV light by 4EP molecules when high 4EP initial concentrations are treated.

Figure 5a shows 4EP and TOC (in mg C/L) decay with time during the treatment of 100 mg/L 4EP aqueous solution by the heterogeneous photo-Fenton process using 1000 mg/L $H_2O_2$, 40 mg/L $Fe_3O_4$ at pH 3 under 300 rpm stirring and room temperature. As it can be seen, 4EP and TOC concentrations decline with time with different rates. As it can be observed, 4EP decay is more rapid than TOC indicating 4EP degradation into intermediates without $CO_2$ release, which undergoes several oxidation steps to mineralize at the end of the treatment. The UV–VIS absorption spectra plotted in Figure 5b confirm the opening of the pyridine ring by the disappearance of the band located at 260 nm after 60 min. HPLC analysis detected the formation of 4-pyridone and 4-hydroxypyridine as aromatic intermediates and maleic and oxalic acids as aliphatic intermediates. Figure 5c presents the changes of the peak area of each intermediate with time during the heterogeneous photo-Fenton treatment of 100 mg/L 4EP aqueous solution. 4-hydroxypyridine and 4-pyridone were formed at the beginning of the treatment and disappeared within 30 min. Maleic acid was detected during the first 60 min, while oxalic acid was accumulated during the treatment. These results confirm the formation of aromatic intermediates, which undergo an opening of the pyridine ring to form aliphatic carboxylic acids (maleic acid and formic acid). The mineralization of organic pollutants containing heteroatoms involves the release of inorganic ions. To obtain more details about the degradation of 4EP by the heterogeneous photo-Fenton oxidation, additional chemical analysis (ion chromatography) was conducted. Figure 5d shows the change of the concentration of nitrates, nitrites, and ammonium ions with time during the treatment of 100 mg/L 4EP by the heterogeneous photo-Fenton process under optimal conditions. The concentration of ammonium increased linearly from the beginning of the treatment to reach a plateau after 60 min. Only small amounts of nitrate and nitrite ions (<0.2 mg/L) were detected. This result indicates that the organic nitrogen contained in 4EP was released stoichiometrically as ammonium ions.

Based on HPLC, ion chromatographic, and TOC analyses, a simple mechanistic scheme can be proposed for the degradation of 4EP by the heterogeneous photo-Fenton process (see Figure 6). 4EP degradation begins by a rapid release of ethyl group as formic acid and its substitution by hydroxyl radical to form 4-pyridone and 4-hydroxypyridine (tautomeric forms). These intermediates undergo oxidative opening of pyridine ring by hydroxyl radicals to form aliphatic carboxylic acids (oxalic and formic acids) and release ammonium ions. Finally, the carboxylic acids end to mineralize into $CO_2$ and $H_2O$ in the final stages of the treatment.

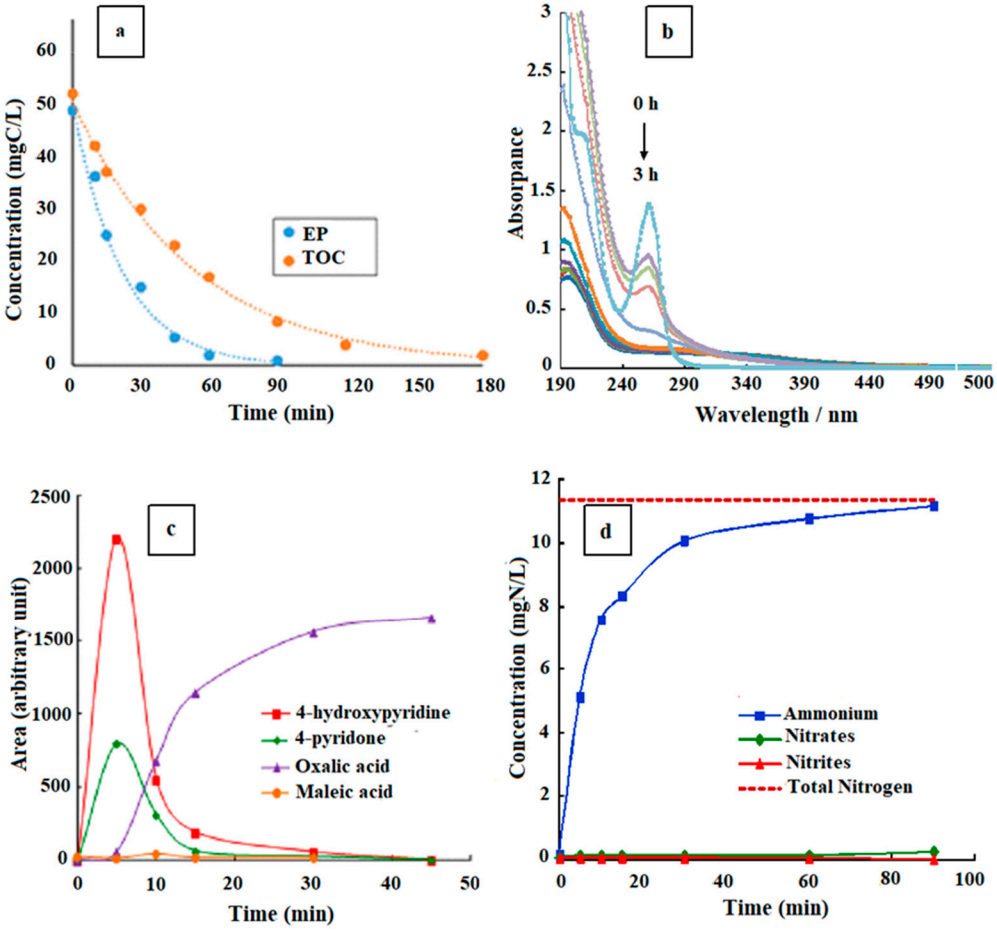


**Figure 5.** Changes with time of (**a**) EP and TOC, (**b**) UV–VIS spectra, (**c**) intermediate HPLC peak areas, and (**d**) speciation of nitrogen during the treatment of 100 mg/L EP aqueous solutions by the heterogeneous photo-Fenton process. Experimental conditions: 1000 mg/L $H_2O_2$, 40 mg /L $Fe_3O_4$, pH 3, T = 25 °C, 300 rpm.

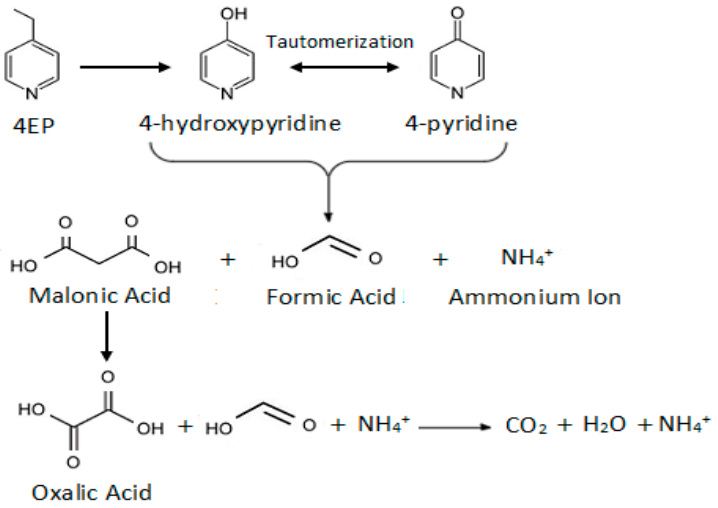


**Figure 6.** Simple mechanistic scheme for nicotinic acid mineralization by the photo-Fenton process.

## 4. Conclusions

The results show that 4EP degradation by the heterogeneous photo-Fenton process ($UV/H_2O_2/Fe_3O_4$) was the most rapid and most efficient among the single processes (UV irradiation,

$Fe_3O_4$ adsorption, and $H_2O_2$ oxidation) and the combined processes (Fenton-like ($H_2O_2/Fe_3O_4$) and UV/$H_2O_2$). This can be explained by higher production of radical species mainly $HO^{\bullet}$ radicals from both the catalytic decomposition of $H_2O_2$ on the surface of $Fe_3O_4$ catalyst, and the photodecomposition of $H_2O_2$ by irradiation UV. The highest TOC removal achieved from 100 mg/L 4EP aqueous solutions by the heterogeneous photo-Fenton process was obtained using 1000 mg/L $H_2O_2$, 40 mg/L $Fe_3O_4$ at pH 3.0 under 300 rpm and room temperature. However, 25% of the total iron contained initially in $Fe_3O_4$ solid catalyst was dissolved in water. The catalyst was collected and heat treated at 105 °C, 180 °C, 250 °C, and 500 °C; then it was reused in the heterogeneous photo-Fenton oxidation of 4EP under the same conditions. The heat-treated catalyst reuse resulted in TOC removals greater than 64%, but the highest TOC removals (>83% after being reused five times) were obtained with the catalyst heat-treated at 500 °C. The detailed mechanistic and kinetic studies demonstrated a pseudo-first order degradation. 4EP degradation involves several stages starting with formation of aromatic intermediates by release of carboxylic group followed by oxidative opening of pyridine ring to form aliphatic carboxylic acids that end to mineralize into $CO_2$, $H_2O$, and $NH_4^+$. These results confirm that the heterogeneous photo-Fenton process could be effectively used to treat wastewaters contaminated with food additives including vitamins. Additionally, treated wastewaters can be recycled in several agricultural and industrial applications and/or reused in landscapes/gardens irrigation systems.

**Author Contributions:** Conceptualization: N.B., A.B., and M.I.A.; methodology: N.B.; validation: M.I.A, A.B., and N.B.; formal analysis: M.I.A. and A.B.; investigation: N.B. and A.B.; resources: N.B.; data curation: M.I.A.; writing—original draft preparation: N.B.; writing—review and editing: A.B. and M.I.A.; supervision: N.B.; project administration: N.B. and A.B.

**Funding:** This research received no external funding.

**Acknowledgments:** The publication of this article was funded by the Qatar National Library.

**Conflicts of Interest:** The authors declare no conflict of interest.

## References

1. Bach, P.; Nilsson, K.; Wallberg, A.; Bauer, U.; Hammerland, L.G.; Peterson, A.; Svensson, T.; Österlund, K.; Karis, D.; Boije, M.; et al. New Series of Pyridinyl-alkynes as Antagonists of the Metabotropic Glutamate Receptor 5 (mGluR5). *Bioorg. Med. Chem. Lett.* **2006**, *16*, 4792–4795. [CrossRef] [PubMed]
2. Agency for Toxic Substances and Disease Registry (ATSDR). *Toxicological Profile for Pyridine*; Department of Health and Human Services, Public Health Service: Atlanta, GA, USA, 1992.
3. International Agency for Research on Cancer (IARC). Pyridine Summary & Evaluation. *IARC IPCS Inchem.* **2000**, *77*, 503.
4. Bhattacharya, S.; Mukherjee, U.K.; Greene, M.I. Method for Making Middle Distillates and a Heavy Vacuum Gas Oil FCC Feedstock. U.S. Patent 9803147B2, USA, 31 October 2017.
5. Sims, G.K.; O'Loughlin, E.J.; Crawford, R.L. Degradation of pyridines in the environment. *Crit. Rev. Environ. Sci. Technol.* **1989**, *19*, 309–340. [CrossRef]
6. Zuo, P.; Shen, W. Identification of nitrogen-polyaromatic compounds in asphaltene from co-processing of coal and petroleum residue using chromatography with mass spectrometry. *Int. J. Coal Sci. Technol.* **2017**, *4*, 281–299. [CrossRef]
7. Shen, J.; Chen, Y.; Wu, S.; Wu, H.; Liu, X.; Sun, X.; Li, J.; Wang, L. Enhanced pyridine biodegradation under anoxic condition: The key role of nitrate as the electron acceptor. *Chem. Eng. J.* **2015**, *277*, 140–149. [CrossRef]
8. Li, N.; Lu, X.; Zhang, S. A novel reuse method for waste printed circuit boards as catalyst for wastewater bearing pyridine degradation. *Chem. Eng. J.* **2014**, *257*, 253–261. [CrossRef]
9. Kong, J.; Wei, X.Y.; Li, Z.K.; Yan, H.L.; Zhao, M.X.; Zong, Z.M. Identification of organonitrogen and organooxygen compounds in the extraction residue from Buliangou subbituminous coal by FTICRMS. *Fuel* **2016**, *171*, 151–158. [CrossRef]
10. Jin, Y.; Yue, Q.; Yang, K.; Wu, S.; Li, S.; Gao, B.; Gao, Y. Pre-treatment of pyridine wastewater by new cathodic–anodic-electrolysis packing. *J. Environ. Sci.* **2018**, *63*, 43–49. [CrossRef]

11. Tabassum, S.A.; Ji, Q.; Hena, S.; Chu, C.; Yu, G.; Zhang, Z. Treatment of coal gasification wastewater by anaerobic SBR–aerobic SBR process for elimination of toxic organic matters-a lab scale study. *RSC Adv.* **2015**, *5*, 58334–58344. [CrossRef]
12. Wang, J.; Jiang, X.; Liu, X.; Sun, X.; Han, W.; Li, J.; Wang, L.; Shen, J. Microbial degradation mechanism of pyridine by *Paracoccus* sp. NJUST30 newly isolated from aerobic granules. *Chem. Eng. J.* **2018**, *344*, 86–94. [CrossRef]
13. Padoley, K.V.; Mudliar, S.N.; Pandey, R.A. Heterocyclic nitrogenous pollutants in the environment and their treatment options–An overview. *Bioresour. Technol.* **2008**, *99*, 4029–4043. [CrossRef] [PubMed]
14. Duan, L.; Li, J.; Shang, K.; Na, L.; Wu, Y. Enhanced biodegradability of coking wastewater by gas phase dielectric barrier discharge plasma. *Sep. Purif. Technol.* **2015**, *154*, 359–365. [CrossRef]
15. Zhu, H.; Han, Y.; Ma, W.; Han, H.; Ma, W. Removal of selected nitrogenous heterocyclic compounds in biologically pretreated coal gasification wastewater (BPCGW) using the catalytic ozonation process combined with the two-stage membrane bioreactor (MBR). *Bioresour. Technol.* **2017**, *245*, 786–793. [CrossRef] [PubMed]
16. Boczkaj, G.; Makoś, P.; Fernandes, A.; Przyjazny, A. New procedure for the examination of the degradation of volatile organonitrogen compounds during the treatment of industrial effluents. *J. Sep. Sci.* **2017**, *40*, 1301–1309. [CrossRef] [PubMed]
17. Yanting, Z.; Junbin, J.; Siqiong, X.; Hongmei, W.; Biao, S.; Jian, H.; Jiguo, Q.; Chen, Q. Biodegradation of Picolinic Acid by *Rhodococcus* sp. PA18. *Appl. Sci.* **2019**, *9*, 1006–1016.
18. Ahmed, B.; Limem, E.; Abdel-Wahab, A.; Nasr, B. Photo-Fenton Treatment of Actual Agro-Industrial Wastewaters. *Ind. Eng. Chem. Res.* **2011**, *50*, 6673–6680. [CrossRef]
19. Bensalah, N.; Dbira, S.; Bedoui, A. The contribution of mediated oxidation mechanisms in the electrolytic degradation of cyanuric acid using diamond anodes. *J. Environ. Sci.* **2016**, *45*, 115–123. [CrossRef]
20. Dbira, S.; Bedoui, A.; Bensalah, N. Investigations on the Degradation of Triazine Herbicides in Water by Photo-Fenton Process. *Am. J. Anal. Chem.* **2014**, *5*, 500–517. [CrossRef]
21. Klavarioti, M.; Mantzavinos, D.; Kassinos, D. Removal of residual pharmaceuticals from aqueous systems by advanced oxidation processes. *Environ. Int.* **2009**, *35*, 402–417. [CrossRef]
22. Bensalah, N.; Bedoui, A.; Chellam, S.; Abdelwahab, A. Electro-Fenton Treatment of Photographic Processing Wastewaters. *Clean–Soil Air Water.* **2013**, *41*, 635–644. [CrossRef]
23. Dbira, S.; Bensalah, N.; Cañizares, P.; Rodrigo, M.A.; Bedoui, A. The electrolytic treatment of synthetic urine using DSA electrodes. *J. Electroanal. Chem.* **2015**, *744*, 62–68. [CrossRef]
24. Barrera-Díaz, C.; Cañizares, P.; Fernández, F.J.; Natividad, R.; Rodrigo, M.A. Electrochemical Advanced Oxidation Processes: An Overview of the Current Applications to Actual Industrial Effluents. *J. Mex. Chem. Soc.* **2014**, *58*, 256–275. [CrossRef]
25. Pérez-Moya, M.; Graells, M.; Castells, G.; Amigó, J.; Ortega, E.; Buhigas, G.; Pérez, L.M.; Mansilla, H.D. Characterization of the degradation performance of the sulfamethazine antibiotic by photo-Fenton process. *Water Res.* **2010**, *44*, 2533–2540. [CrossRef] [PubMed]
26. Vilar, V.J.; Rocha, E.M.; Mota, F.S.; Fonseca, A.; Saraiva, I.; Boaventura, R.A. Treatment of a sanitary landfill leachate using combined solar photo-Fenton and biological immobilized biomass reactor at a pilot scale. *Water Res.* **2011**, *45*, 2647–2658. [CrossRef] [PubMed]
27. Zhang, X.; He, M.; Liu, J.H.; Liao, R.; Zhao, L.; Xie, J.; Wang, R.; Yang, S.; Wang, H.; Liu, Y. $Fe_3O_4$@C nanoparticles as high-performance Fenton-like catalyst for dye decoloration. *Sci. Bull.* **2014**, *59*, 3406–3412. [CrossRef]
28. Garrido-Ramirez, E.G.; Theng, B.K.; Mora, M.L. Clays and oxide minerals as catalysts and nanocatalysts in Fenton-like reactions—A review. *Appl. Clay Sci.* **2010**, *47*, 182–192. [CrossRef]
29. Xia, M.; Long, M.; Yang, Y.; Chen, C.; Cai, W.; Zhou, B. A highly active bimetallic oxides catalyst supported on Al-containing MCM-41 for Fenton oxidation of phenol solution. *Appl. Catal. B Environ.* **2011**, *110*, 118–125. [CrossRef]
30. Li, P.; Xu, H.Y.; Li, X.; Liu, W.C.; Li, Y. Preparation and Evaluation of a Photo-Fenton Heterogeneous Catalyst: Spinel-typed $ZnFe_2O_4$. *J. Adv. Mater. Res.* **2012**, *550–553*, 329–335. [CrossRef]
31. Wu, Y.; Chen, R.; Liu, H.; Wei, Y.; Wu, D. Feasibility and mechanism of p-nitrophenol decomposition in aqueous dispersions of ferrihydrite and $H_2O_2$ under irradiation. *React. Kinet. Mech. Cat.* **2013**, *110*, 87–99. [CrossRef]

32. Sun, P.; Lemley, A.T. P-Nitrophenol degradation by a heterogeneous Fenton-like reaction on nano-magnetite: Process optimization, kinetics, and degradation pathways. *J. Mol. Catal. A Chem.* **2011**, *349*, 71–79. [CrossRef]
33. Nidheesh, P.V. Heterogeneous Fenton catalysts for the abatement of organic pollutants from aqueous solution: A review. *RSC Adv.* **2015**, *5*, 40552–40577. [CrossRef]
34. Hongping, H.E.; Zhong, Y.; Liaang, X.; Tan, W.; Zhu, J.; Wang, C.Y. Natural Magnetite: An efficient catalyst for the degradation of organic contaminant. *Sci. Rep.* **2015**, *5*, 10139.
35. Bai, Z.; Yang, Q.; Wang, J. Degradation of sulfamethazine antibiotics in Fenton-like system using $Fe_3O_4$ magnetic nanoparticles as catalyst. *Environ. Prog. Sustain.* **2017**, *36*, 1743–1753. [CrossRef]
36. Chen, F.; Xie, S.; Huang, X.; Qiu, X. Ionothermal synthesis of $Fe_3O_4$ magnetic nanoparticles as efficient heterogeneous Fenton-like catalysts for degradation of organic pollutants with $H_2O_2$. *J. Hazard. Mater.* **2017**, *322*, 152–162. [CrossRef]
37. Yang, S.S.; Wu, P.; Yang, Q.; Zhu, N.; Lu, G.; Dang, Z. Regeneration of iron-montmorillonite adsorbent as an efficient heterogeneous Fenton catalytic for degradation of Bisphenol A: Structure, performance and mechanism. *Chem. Eng. J.* **2017**, *328*, 737–747. [CrossRef]
38. Pourzamani, H.; Hajizadeh, Y.; Mengelizadeh, N. Application of three-dimensional electrofenton process using MWCNTs-$Fe_3O_4$ nanocomposite for removal of diclofenac. *Process. Saf. Environ.* **2018**, *119*, 271. [CrossRef]
39. Nogueira, A.E.; Castro, I.A.; Giroto, A.S.; Magriotis, Z.M. Heterogeneous Fenton-Like Catalytic Removal of Methylene Blue Dye in Water Using Magnetic Nanocomposite (MCM-41/Magnetite). *J. Catal.* **2014**, *2014*, 1–6. [CrossRef]
40. Dehghani, M.; Taghizadeh, M.M.; Gholami, T.; Ghadami, M.; Keshtgar, L.; Elhameyan, Z.; Javaheri, M.R.; Shamsedini, N.; Jamshidi, F.; Shahsavani, S.; et al. Optimization of the Parameters Influencing the Photo-Fenton Process for the Decolorization of Reactive Red 198 (RR198). *Jentashapur J. Health Sci.* **2015**, *7*, 28243. [CrossRef]
41. Matos, T.A.F.; Dias, A.L.N.; Reis, A.D.P.; Silva, M.R.A.d.; Kondo, M.M. Degradation of Abamectin Using the Photo-Fenton Process. *Int. J. Chem. Eng.* **2012**, *2012*, 1–7. [CrossRef]
42. Ahmed, B.; Mohamed, H.; Limem, E.; Nasr, B. Degradation and Mineralization of Organic Pollutants Containedin Actual Pulp and Paper Mills Wastewaters by a UV/$H_2O_2$ Process. *Ind. Eng. Chem. Res.* **2009**, *48*, 3370–3379. [CrossRef]
43. Lutterbeck, C.A.; Wilde, M.L.; Baginska, E.; Leder, C.; Machado, Ê.L.; Kümmerer, K. Degradation of 5-FU by means of advanced (photo) oxidation processes: UV/$H_2O_2$, UV/$Fe^{2+}$/$H_2O_2$ and UV/$TiO_2$—Comparison of transformation products, ready biodegradability and toxicity. *Sci. Total Environ.* **2015**, *527*, 232–245. [CrossRef]
44. Biglari, H.; Kord, M.F.; Joneidi, J.A.; Bazrafshan, E. Removal of Humic acid from environmental aqueous by Fenton Oxidation Process. *J. North Khorasan Univ. Med. Sci.* **2013**, *5*, 37–45. [CrossRef]
45. Klamerth, N.; Malato, S.; Maldonado, M.I.; Aguera, A.; Fernández-Alba, A.R. Application of Photo-Fenton as a Tertiary Treatment of Emerging Contaminants in Municipal Wastewater. *Environ. Sci. Technol.* **2010**, *44*, 1792–1798. [CrossRef]
46. Daneshvar, N.; Khataee, A.R. Removal of azo dye C.I. acid red 14 from contaminated water using Fenton, UV/$H_2O_2$, UV/$H_2O_2$/Fe(II), UV/$H_2O_2$/Fe(III) and UV/$H_2O_2$/Fe(III)/oxalate processes: A comparative study. *J. Environ. Sci. Health A* **2006**, *41*, 315–328. [CrossRef]
47. Dehghani, M.; Shahsavani, S.; Shamsedini, N.; Javaheri, M.R. Removal of nitrate from aqueous solution using rice chaff. *Jentashapir J. Health Res.* **2015**, *6*, 22–26. [CrossRef]
48. Zheng, H.; Pan, Y.; Xiang, X. Oxidation of acidic dye Eosin Y by the solar photo-Fenton processes. *J. Hazard. Mater.* **2007**, *141*, 457–464. [CrossRef]